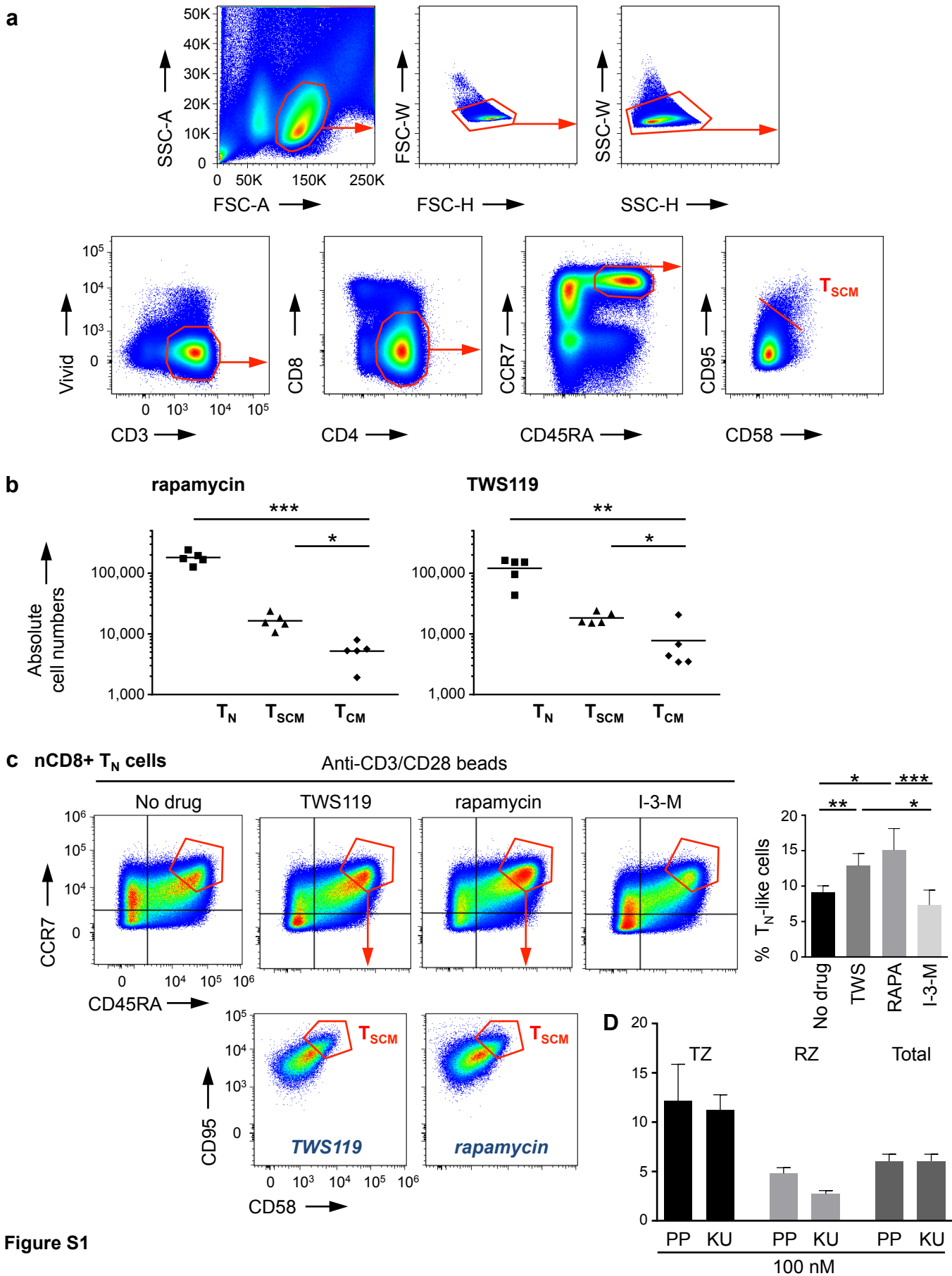


Scholz et al.:

**MODULATION OF mTOR SIGNALLING  
TRIGGERS THE FORMATION OF STEM CELL-LIKE MEMORY T CELLS**

**SUPPLEMENTAL INFORMATION**



## Figure S1

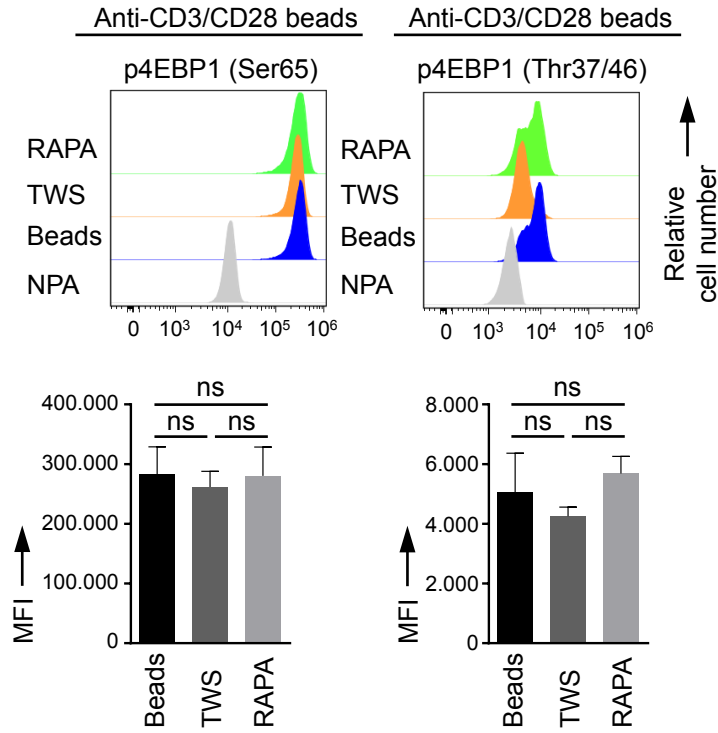
(a) Gating strategy for the phenotypic detection of human  $T_{SCM}$  cells (here shown for  $CD4^+$   $T_{SCM}$  cells): Lymphocytes  $\rightarrow$  Doublet exclusion (FSC and SSC)  $\rightarrow$  Live  $CD3^+$  T cells  $\rightarrow$   $CD4^+$ ,  $CD8^-$  T cells  $\rightarrow$   $CCR7^+$ ,  $CD45RA^+$  T cells  $\rightarrow$   $CD95^-$ ,  $CD58^-$   $T_N$  cells (when sorted, termed highly purified) and  $CD95^+$ ,  $CD58^+$   $T_{SCM}$  cells. FSC = forward scatter. SSC = side scatter. A = area. H = height. W = width.  $T_{SCM} = T_{SCM}$  cells.

(b) Absolute cell numbers in the small-sized lymphocyte population. 14 day-long priming of 1,000,000  $nCD4^+$   $T_N$  cells in the presence of rapamycin or TWS119 specifically induces  $T_{SCM}$  cells, verified by assessment of the absolute cell numbers in the cell culture. Rapamycin (left) and TWS119 (right) significantly increase the numbers of  $T_{SCM}$  cells in comparison to  $T_{CM}$  cells.  $T_N = T_N$ -like cells.  $T_{SCM} =$  pharmacologically induced  $T_{SCM}$  cells.  $T_{CM} = T_{CM}$ -like cells.  $n = 5$ .

(c) TWS119 and rapamycin induce phenotypic  $CD8^+$   $T_{SCM}$  cells. Highly purified phenotypic  $nCD8^+$   $T_{SCM}$  cells, activated for 14 days in the presence of TWS119 (5  $\mu$ M) or rapamycin (100 nM) exhibit increased  $CCR7^+$ ,  $CD45RA^+$   $T_N$ -like cell frequencies (gated on live  $CD3^+$ ,  $CD8^+$  T cells), containing phenotypic  $CD95^+$ ,  $CD58^+$   $T_{SCM}$  cells. When  $nCD8^+$   $T_N$  cells were cultured in the absence of TWS119 or rapamycin or on the presence of Indirubin-3-monoxime (I-3-M, 4  $\mu$ M) they did not display increased  $T_N$ -like cell frequencies.  $T_N$ -like cell frequencies are depicted as percentage of live  $CD3^+$ ,  $CD8^+$  T cells.  $T_{SCM} =$  pharmacologically induced  $T_{SCM}$  cells. TWS = TWS119. RAPA = rapamycin.  $n = 4$ .

(d) Phenotypic  $CD95^+$ ,  $CD58^+$   $T_{SCM}$  cells in the TZ (transition zone), RZ (rand zone) and total  $T_N$ -like cell population after activation of highly purified human  $nCD4^+$   $T_N$  cells for 14 days in the presence of PP242 (100 nM) or KU-0063794 (100 nM).  $T_{SCM}$  cell frequencies are depicted as percentages of the defined zones. Data are represented as mean  $\pm$  SEM.  $n = 4$ . PP = PP242. KU = KU-0063794.

**a** nCD4+ T<sub>N</sub> cells



**b** nCD8+ T<sub>N</sub> cells

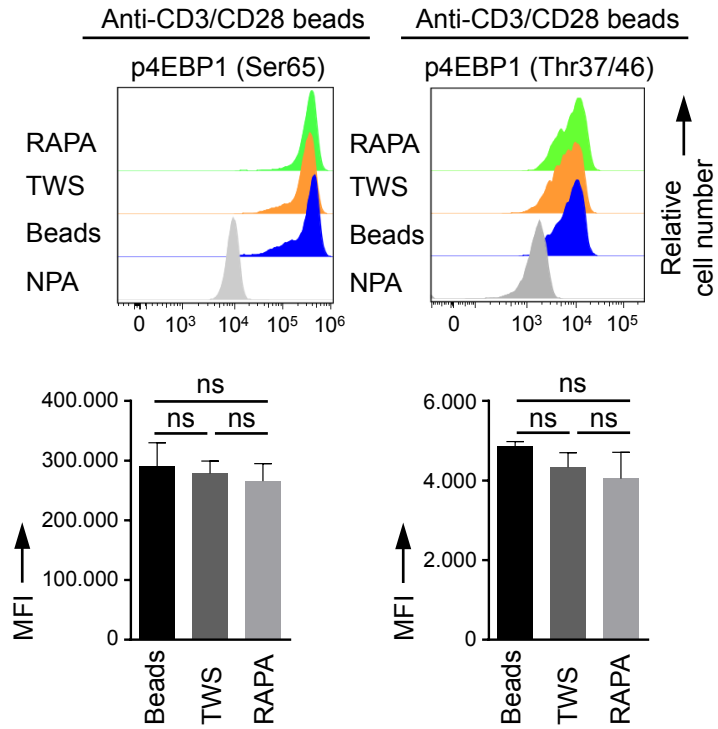


Figure S2

## Figure S2

Assessment of 4EBP1 phosphorylation by flow cytometry.

TWS119 (5  $\mu$ M) and rapamycin (100 nM) have no significant effects on the phosphorylation of 4EBP1 (Ser65 and Thr37/46) in (a) highly purified (T<sub>SCM</sub> cell-freed), activated human nCD4<sup>+</sup> T<sub>N</sub> cells and in (b) highly purified, activated human nCD8<sup>+</sup> T<sub>N</sub> cells. NPA = no primary antibody. Beads = anti-CD3/CD28 beads. TWS = TWS119. RAPA = rapamycin. MFI = Median Fluorescence Intensity. n = 3.

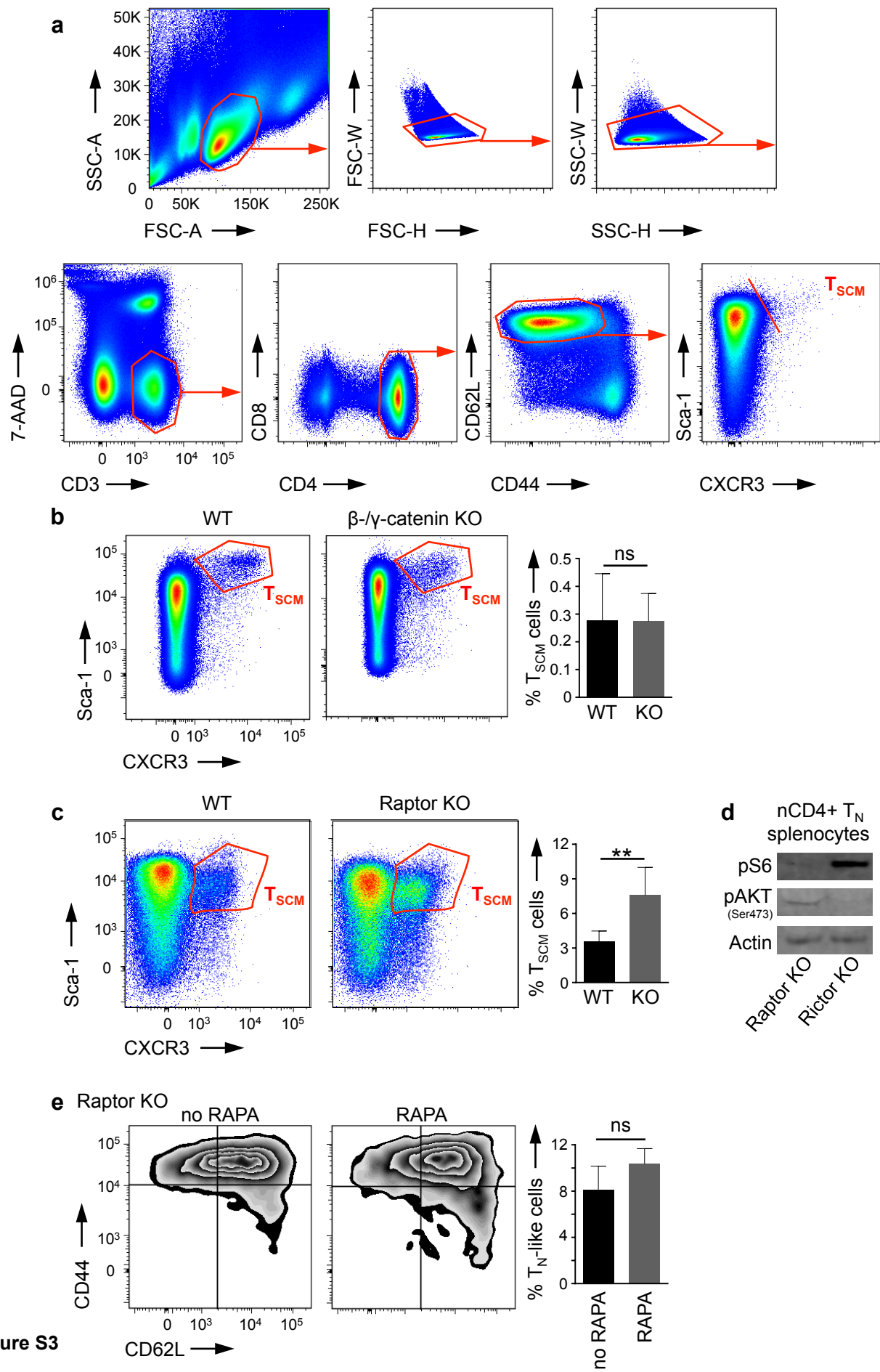


Figure S3

### Figure S3

(a) Gating strategy for the phenotypic detection of mouse  $T_{SCM}$  cells (here shown for CD4<sup>+</sup> T cells): Lymphocytes → Doublet exclusion (FSC and SSC) → Live CD3<sup>+</sup> T cells → CD4<sup>+</sup>, CD8<sup>-</sup> T cells → CD62L<sup>+</sup>, CD44<sup>-</sup> T cells → CXCR3<sup>-</sup>, Sca-1<sup>-</sup>  $T_N$  cells (when sorted, termed highly purified) and CXCR3<sup>+</sup>, Sca-1<sup>+</sup>  $T_{SCM}$  cells. FSC = forward scatter. SSC = side scatter. A = area. H = height. W = width.  $T_{SCM}$  =  $T_{SCM}$  cells.

(b) Mice with haematopoietic deletion of  $\beta$ - and  $\gamma$ -catenin display naturally occurring  $T_{SCM}$  cells.

Similar frequencies of Sca-1<sup>+</sup>, CXCR3<sup>+</sup>, CD44<sup>-</sup>, CD62L<sup>+</sup> naturally occurring  $T_{SCM}$  cells in mice with haematopoietic knockout (KO) of  $\beta$ - and  $\gamma$ -catenin as in their wild-type (WT) counterparts (gated on live CD3<sup>+</sup>, CD4<sup>+</sup>, CD44<sup>-</sup>, CD62L<sup>+</sup> T cells).  $T_{SCM}$  cell frequencies are depicted as percentage of live CD3<sup>+</sup>, CD4<sup>+</sup>, CD44<sup>-</sup>, CD62L<sup>+</sup> T cells. Data are represented as mean  $\pm$  SEM.  $T_{SCM}$  = naturally occurring  $T_{SCM}$  cells. n = 3.

(c) Mice with T cell-specific deletion of Raptor display increased  $T_{SCM}$  cell frequencies.

Increased frequencies of naturally occurring Sca-1<sup>+</sup>, CXCR3<sup>+</sup>, CD44<sup>-</sup>, CD62L<sup>+</sup>  $T_{SCM}$  cells in mice with T cell-specific knockout (KO) of Raptor compared to their wild-type (WT) counterparts (gated on live CD3<sup>+</sup>, CD44<sup>-</sup>, CD62L<sup>+</sup> T cells).  $T_{SCM}$  cell frequencies are depicted as percentage of live CD3<sup>+</sup>, CD44<sup>-</sup>, CD62L<sup>+</sup> T cells. Data are represented as mean  $\pm$  SEM.  $T_{SCM}$  = naturally occurring  $T_{SCM}$  cells. n = 9.

(d) Assessment of S6 and AKT (Ser473) phosphorylation in mice with either a T cell-specific knockout (KO) of Raptor or of Rictor by Western blot technique.

Mice with T cell-specific KO of Raptor display decreased phosphorylation of S6, but phosphorylation of AKT (Ser473) in highly purified nCD4<sup>+</sup>  $T_N$  cells, indicating inhibition of mTORC1 and simultaneous activity of mTORC2. Highly purified nCD4<sup>+</sup>  $T_N$  cells from mice with T cell-specific KO of Rictor show the opposite. n = 5.

(e) Treatment of Raptor KO nCD4<sup>+</sup>  $T_N$  cells with rapamycin.

Treatment of Raptor KO nCD4<sup>+</sup>  $T_N$  cells during 4-day priming with rapamycin (100 nM) does not result in an increased fraction of  $T_N$ -like phenotype cells. RAPA = rapamycin. n = 3.

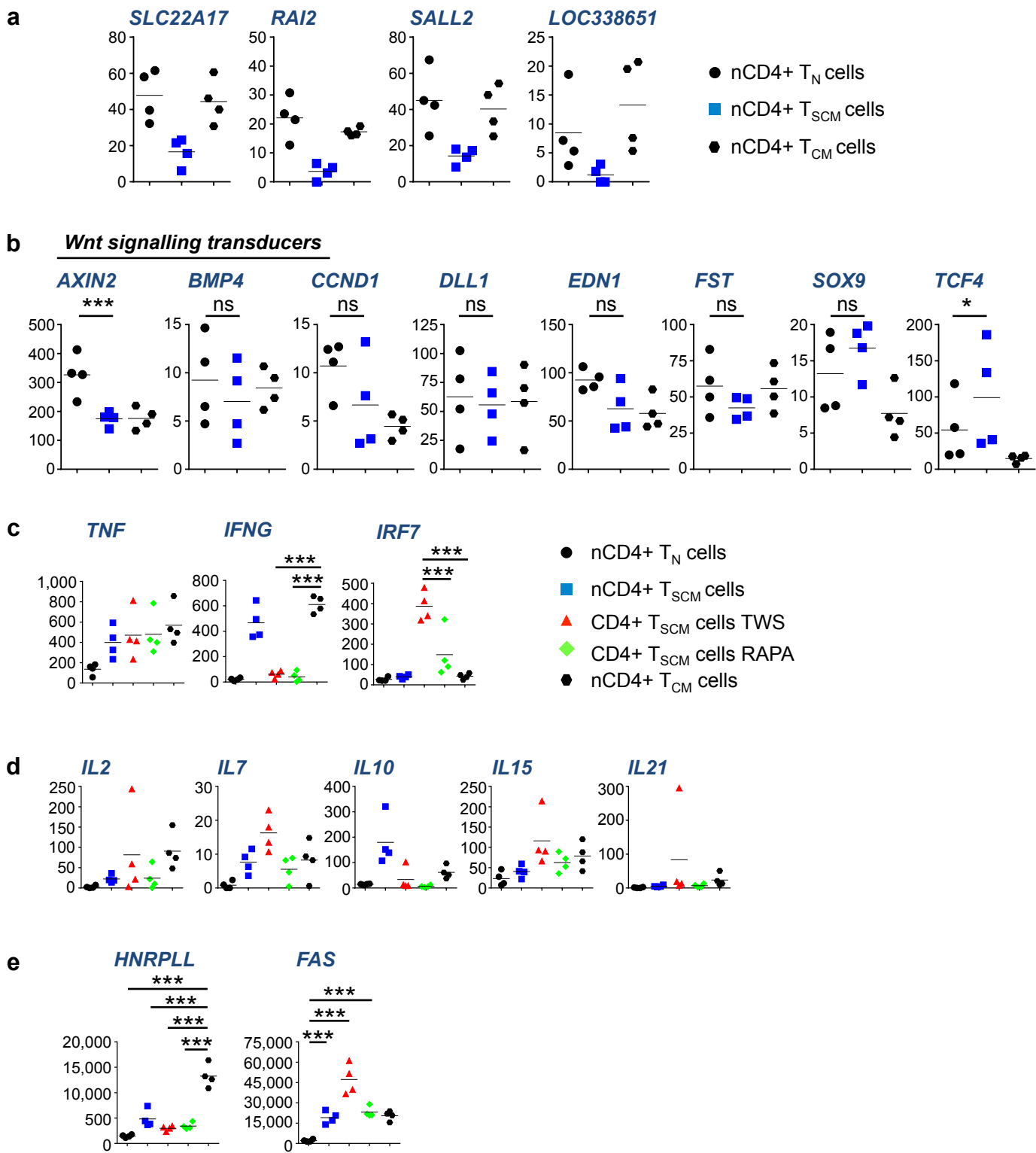


Figure S4



#### Figure S4

(a) Gene expression profiles of *SLC22A17*, *RAI2*, *SALL2* and *LOC338651* in nCD4<sup>+</sup> T<sub>SCM</sub> cells.

From the set of 56 genes which show a unique expression profile in nCD4<sup>+</sup> T<sub>SCM</sub> cells (Table 1), only 4, namely *SLC22A17*, *RAI2*, *SALL2* and *LOC338651*, are found to be significantly down-regulated in nCD4<sup>+</sup> T<sub>SCM</sub> cells in comparison to nCD4<sup>+</sup> T<sub>N</sub> cells and nCD4<sup>+</sup> T<sub>CM</sub> cells.

(b) Gene expression profiles of Wnt signalling transducers in nCD4<sup>+</sup> T<sub>N</sub> cells and nCD4<sup>+</sup> T<sub>SCM</sub> cells.

Widespread similar expression of genes encoding transducers of Wnt signalling in nCD4<sup>+</sup> T<sub>N</sub> cells and nCD4<sup>+</sup> T<sub>SCM</sub> cells.

(c) Gene expression profiles of the genes encoding *TNF*, *IFNG* and *IRF7*.

(d) Gene expression profiles of the genes encoding *IL2*, *IL7*, *IL10*, *IL15* and *IL21*.

(e) Gene expression profile of the genes of the key regulator of the alternative splicing of the CD45 pre-mRNA, *HNRPLL*, and of *FAS*.

Data are based on transcriptome analysis in 4 healthy human individuals. The y-axes show normalized counts. TWS = TWS119-induced T<sub>SCM</sub> cells. RAPA = rapamycin-induced T<sub>SCM</sub> cells.

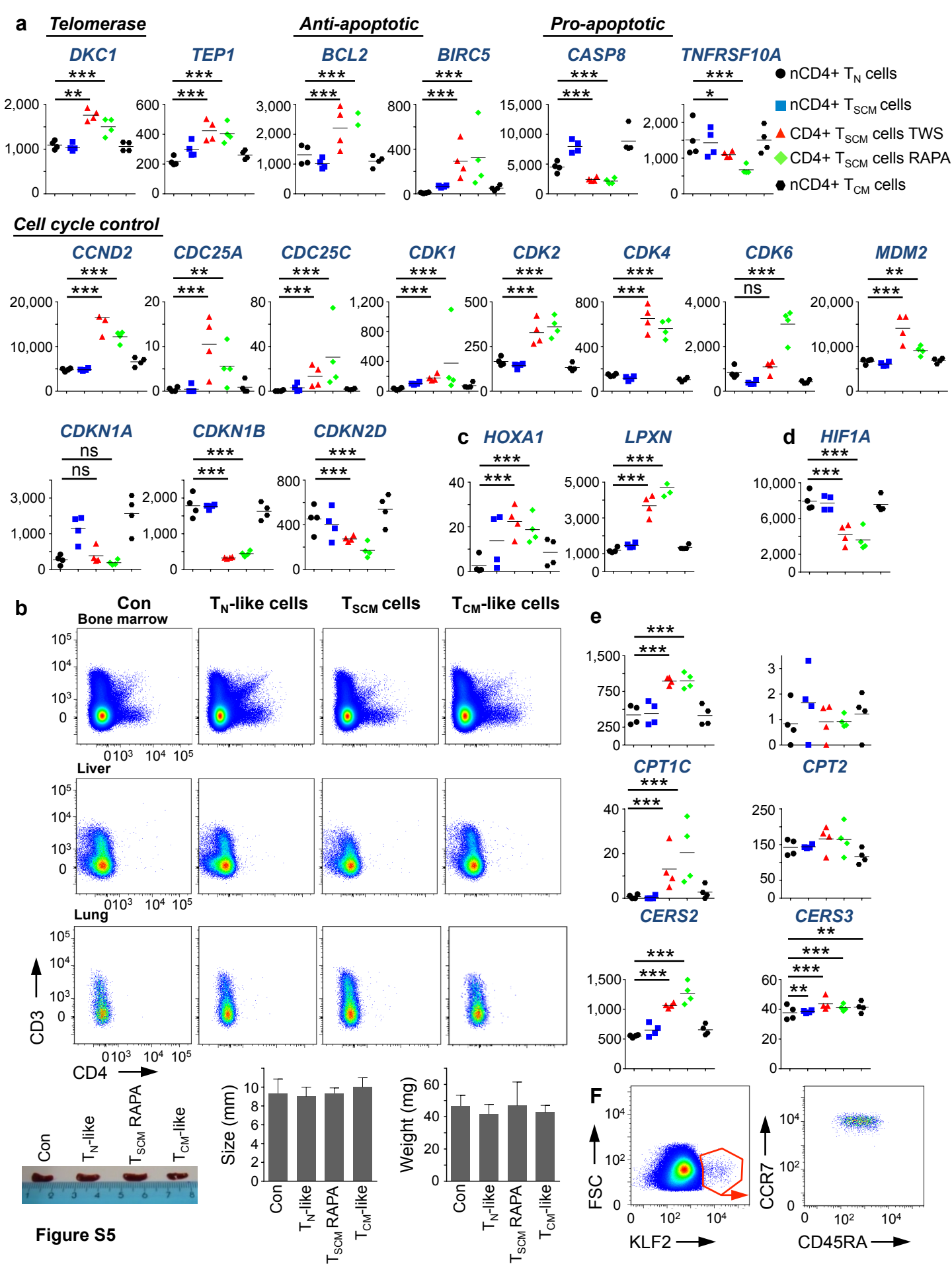


Figure S5

## Figure S5

(a) Gene expression profiles of genes involved in cell cycle control.

Rapamycin-induced CD4<sup>+</sup> T<sub>SCM</sub> cells exhibit an expression profile of genes involved in the regulation of cell death, longevity and cell cycle control, suggesting that they are equipped with a superior long-term survival capacity.

(b) *In vivo* long-term repopulation capacity of rapamycin-induced CD4<sup>+</sup> T<sub>SCM</sub> cells.

No live CD3<sup>+</sup>, CD4<sup>+</sup> T cells could be detected in the bone marrow, liver and lung of NSG mice after adoptive transfer. Con = control: injection of 200 µl cell culture medium. The spleens of the adoptively transferred NSG mice did not display differences in size or weight with respect to the adoptively transferred T cell subset. n = 3.

(c) Gene expression profiles of engraftment genes in *in vitro* induced T<sub>SCM</sub> cells.

Up-regulation of *HOXA1* and *LPXN* in rapamycin-induced CD4<sup>+</sup> T<sub>SCM</sub> cells and of *HOXA1* in naturally occurring CD4<sup>+</sup> T<sub>SCM</sub> cells.

(d) Glucose uptake in CD4<sup>+</sup> T cell subsets.

Low expression levels of *HIFA* pharmacologically induced CD4<sup>+</sup>T<sub>SCM</sub> cells.

(e) Gene expression profiles of carnitine palmitoyl transferases and ceramide synthases.

Naturally occurring and pharmacologically induced CD4<sup>+</sup> T<sub>SCM</sub> cells display a characteristic gene expression profile of the genes encoding carnitine palmitoyl transferases (CPT) and ceramide synthases (CERS). Also view the expression of *CERS6* in Figure 5D.

(f) Expression of KLF2 in nCD4<sup>+</sup> T<sub>N</sub> cells.

Only a small fraction of naturally occurring live CD3<sup>+</sup>, CD4<sup>+</sup>, CCR7<sup>+</sup>, CD45RA<sup>+</sup> T<sub>N</sub> cells expresses KLF2 (left). KLF2 expressing nCD4<sup>+</sup> T<sub>N</sub> cells are homogeneously CCR7<sup>+</sup>, CD45RA<sup>+</sup> double positive T cells (right). n = 3.

(a), (c), (d) and (e): Data are based on transcriptome analysis in 4 healthy human individuals. The y-axes show normalized counts. TWS = TWS119-induced CD4<sup>+</sup> T<sub>SCM</sub> cells. RAPA = rapamycin-induced CD4<sup>+</sup> T<sub>SCM</sub> cells.

**Table S1:** Relative percentage and absolute cell number of live CD4+ T<sub>N</sub>, T<sub>SCM</sub>, T<sub>CM</sub> cells and T<sub>EM</sub> cells in the large-sized lymphocyte population. Numbers are presented as mean ± standard error of the mean (SEM). n = 5.

	<i>Beads</i>		<i>rapamycin</i>		<i>TWS119</i>	
	%	absolute	%	absolute	%	absolute
<b>T<sub>N</sub></b>	30.79 ± 5.31	576.015 ± 95.234	24.53 ± 3.93	751.889 ± 273.219	16.33 ± 3.06	324.197 ± 118.263
<b>T<sub>SCM</sub></b>	0.15 ± 0.05	3.627 ± 1.892	0.28 ± 0.11	10.198 ± 5.772	0.14 ± 0.05	4.160 ± 2210
<b>T<sub>CM</sub></b>	31.88 ± 6.15	781.579 ± 296.358	37.82 ± 4.58	1.103.000 ± 351.570	39.32 ± 2.65	956.886 ± 380.725
<b>T<sub>EM</sub></b>	10.20 ± 3.56	223.432 ± 123.831	14.92 ± 2.51	461.691 ± 188.073	21.61 ± 6.31	543.628 ± 344.107

**Table S2:** The 25 top-ranked (by adjusted p-value) significantly differentially expressed genes between nCD4+ T<sub>N</sub> cells and nCD4+ T<sub>SCM</sub> cells.

Up-regulated in T <sub>SCM</sub> cells			Down-regulated in T <sub>SCM</sub> cells		
<i>Gene name</i>	<i>log2FC</i>	<i>adj. p</i>	<i>Gene name</i>	<i>log2FC</i>	<i>adj. p</i>
1. <b>SAMSN1</b>	-1,8720285	2,74E-179	1. <b>IGF1R</b>	1,427881915	2,31E-106
2. <b>LINC00152</b>	-4,0839451	9,51E-122	2. <b>ITGA6</b>	1,231727997	2,92E-74
3. <b>CCR6</b>	-5,3922914	6,95E-119	3. <b>EEA1</b>	1,230984185	9,09E-56
4. <b>RNF19A</b>	-1,6260319	4,17E-117	4. <b>FAM46A</b>	1,066686583	4,69E-34
5. <b>S100A4</b>	-1,7347476	8,23E-108	5. <b>ACPL2</b>	1,381638941	2,89E-29
6. <b>ADAM19</b>	-5,3566214	2,86E-101	6. <b>NR3C2</b>	1,018553372	1,23E-26
7. <b>STAM</b>	-1,8600099	3,13E-92	7. <b>SORCS3</b>	1,780891951	2,97E-26
8. <b>FAM129A</b>	-4,8305544	1,73E-90	8. <b>SFMBT2</b>	1,107115196	1,60E-25
9. <b>SYT11</b>	-3,4862738	1,12E-87	9. <b>ANKRD55</b>	1,268831037	1,76E-23
10. <b>TIGIT</b>	-5,0768887	1,39E-85	10. <b>KRT73</b>	1,802570768	1,60E-20
11. <b>MAF</b>	-2,9002404	1,75E-81	11. <b>LRRC16A</b>	1,046216571	3,19E-20
12. <b>ANXA2</b>	-3,437778	4,21E-75	12. <b>SDK2</b>	1,598688716	3,31E-20
13. <b>KLRB1</b>	-4,3849081	2,92E-74	13. <b>ACVR2B</b>	1,256880619	4,58E-20
14. <b>DUSP4</b>	-4,4591383	3,83E-73	14. <b>LCLAT1</b>	1,102964862	6,65E-20
15. <b>FAS</b>	-3,1098147	2,74E-72	15. <b>PLAG1</b>	1,483654292	2,56E-19
16. <b>ARAP2</b>	-1,4998584	2,17E-68	16. <b>PCSK5</b>	1,395119208	5,54E-19
17. <b>RUNX3</b>	-1,6754918	6,76E-68	17. <b>TRABD2A</b>	1,314541925	7,60E-19
18. <b>COTL1</b>	-1,4702624	1,21E-66	18. <b>ZNF516</b>	1,632620207	1,03E-18
19. <b>CD74</b>	-1,6687414	3,74E-65	19. <b>EGR1</b>	1,159124848	2,25E-18
20. <b>CXCR5</b>	-2,905313	6,71E-60	20. <b>EMR4P</b>	1,404969196	9,00E-18
21. <b>PDIA6</b>	-2,1070971	2,60E-59	21. <b>TSEN2</b>	1,330122989	9,55E-18
22. <b>ITGB1</b>	-2,9217569	3,56E-53	22. <b>RBM11</b>	1,344951381	1,08E-17
23. <b>IL18R1</b>	-2,1791794	1,03E-52	23. <b>DEPDC7</b>	1,975226806	2,32E-17
24. <b>TOP2A</b>	-2,9015196	1,27E-52	24. <b>PLEKHH2</b>	1,533851363	2,57E-17
25. <b>MIAT</b>	-2,7683017	6,62E-52	25. <b>KRT72</b>	1,976578231	8,22E-17

**Table S3:** The 25 top-ranked (by adjusted p-value) significantly differentially expressed genes between nCD4+ T<sub>SCM</sub> and T<sub>CM</sub> cells.

Up-regulated in T <sub>SCM</sub> cells			Down-regulated in T <sub>SCM</sub> cells		
<i>Gene name</i>	<i>log2FC</i>	<i>adj. p</i>	<i>Gene name</i>	<i>log2FC</i>	<i>adj. p</i>
1. <b>HBB</b>	-6,0411627	4,65E-129	1. <b>DST</b>	1,05616476	1,93E-22
2. <b>GZMA</b>	-2,2912417	1,79E-46	2. <b>NAB1</b>	1,25297626	3,21E-19
3. <b>RTKN2</b>	-1,2929428	1,91E-25	3. <b>CXCR5</b>	1,02118417	2,16E-12
4. <b>RBMS3</b>	-2,0342402	1,30E-17	4. <b>HNRPLL</b>	1,37267746	7,85E-09
5. <b>PECAM1</b>	-1,9106633	1,79E-17	5. <b>IL2</b>	1,74024059	9,33E-09
6. <b>BANK1</b>	-3,4515431	4,20E-17	6. <b>NETO2</b>	1,41658235	6,98E-08
7. <b>IKZF2</b>	-1,7893613	3,57E-15	7. <b>LOC100128420</b>	1,49411931	1,15E-06
8. <b>HBA2</b>	-3,100931	4,00E-13	8. <b>KLRB1</b>	1,14802413	2,85E-06
9. <b>CD38</b>	-1,4179443	6,65E-13	9. <b>SMAD5</b>	1,02779121	6,39E-05
10. <b>NKG7</b>	-2,6249869	1,55E-11	10. <b>CCR6</b>	1,21155421	9,57E-05
11. <b>ENC1</b>	-1,2340584	3,52E-11	11. <b>CYP24A1</b>	1,51420011	9,78E-05
12. <b>LAYN</b>	-2,1747497	3,53E-11	12. <b>LOC100505676</b>	1,46485435	0,00019599
13. <b>CNR2</b>	-2,8348965	6,63E-11	13. <b>SLC22A17</b>	1,19257275	0,00213168
14. <b>HLA-DMA</b>	-1,3576176	1,13E-10	14. <b>KCNQ3</b>	1,55002485	0,00254751
15. <b>FCRL2</b>	-2,7184507	5,98E-10	15. <b>H1F0</b>	1,00909404	0,00261769
16. <b>CRTAM</b>	-2,1784364	1,78E-09	16. <b>CDR1</b>	1,47957064	0,0051696
17. <b>GZMK</b>	-1,5935992	1,78E-09	17. <b>LOC338651</b>	1,47185677	0,00535925
18. <b>IGLL5</b>	-2,6436633	2,34E-09	18. <b>ELOVL4</b>	1,25441341	0,00553021
19. <b>MYB</b>	-2,0440295	4,55E-09	19. <b>NPDC1</b>	1,0812657	0,00589619
20. <b>SLAMF7</b>	-2,137982	1,63E-08	20. <b>SALL2</b>	1,13254525	0,00921469
21. <b>KIAA0101</b>	-1,4027786	1,95E-08	21. <b>LOC339894</b>	1,17366326	0,01070789
22. <b>AFF3</b>	-1,0652742	2,44E-08	22. <b>CDS1</b>	1,00968714	0,01255335
23. <b>HLA-DMB</b>	-1,9413391	4,75E-08	23. <b>TBC1D8B</b>	1,13488974	0,01538873
24. <b>DTHD1</b>	-1,8741905	6,89E-08	24. <b>RAI2</b>	1,29395937	0,01762307
25. <b>HBA1</b>	-2,2914809	6,23E-07	25. <b>KIAA1598</b>	1,08462698	0,02564904

**Table S4:** Genes found to be significantly differentially expressed between nCD4<sup>+</sup> T<sub>SCM</sub> and T<sub>CM</sub> cells (ranked by adjusted p-value), but not in any other comparison among the naturally occurring T cell subsets.

*Gene name*

1. **CD38**
2. **ENC1**
3. **AFF3**
4. **AKR1C3**
5. **FGFBP2**
6. **SMAD5**
7. **KIAA0125**
8. **IRF8**
9. **H1F0**
10. **CA1**
11. **CCRL2**
12. **CTBP2**
13. **CDS1**
14. **TBC1D8B**
15. **FGFBP3**
16. **VWDE**
17. **ABCB4**
18. **TCEAL2**

**Table S5:** The 25 top-ranked (by adjusted p-value) significantly differentially expressed genes between rapamycin- and TWS119-induced CD4<sup>+</sup> T<sub>SCM</sub> cells.

Up-regulated in rapamycin-induced T <sub>SCM</sub> cells			Up-regulated in TWS119-induced T <sub>SCM</sub> cells		
<i>Gene name</i>	<i>log2FC</i>	<i>adj. p</i>	<i>Gene name</i>	<i>log2FC</i>	<i>adj. p</i>
1. <b>NQO1</b>	-2,8730812	1,10E-121	1. <b>LAMP3</b>	3,56551112	1,04E-130
2. <b>CDK6</b>	-1,4605378	2,00E-67	2. <b>IFIT3</b>	4,92954195	1,19E-118
3. <b>SPIN1</b>	-1,2016612	2,45E-47	3. <b>USP18</b>	3,0647312	7,79E-93
4. <b>KLHL24</b>	-1,4391299	3,28E-46	4. <b>IFI27</b>	6,20694105	8,40E-88
5. <b>TXNRD1</b>	-1,1725384	1,11E-43	5. <b>IFI6</b>	2,89648652	8,70E-86
6. <b>AHI1</b>	-1,7503645	6,14E-42	6. <b>TLR7</b>	4,21238707	1,53E-79
7. <b>TPCN1</b>	-1,3928224	4,63E-40	7. <b>RASGRP3</b>	2,29468472	3,11E-72
8. <b>IRF2BP2</b>	-1,2786665	3,24E-36	8. <b>HERC5</b>	2,01162857	6,16E-72
9. <b>LOC100128420</b>	-2,4644944	1,77E-30	9. <b>PARP12</b>	1,46461934	6,17E-67
10. <b>LAYN</b>	-2,2649444	2,24E-29	10. <b>JAK2</b>	1,69870158	1,30E-62
11. <b>B3GALNT1</b>	-2,2620449	7,36E-29	11. <b>IFIT2</b>	3,41258634	6,20E-52
12. <b>CSF2RB</b>	-4,0303569	7,69E-29	12. <b>OAS3</b>	2,54400792	1,47E-51
13. <b>IL2RA</b>	-1,3568667	1,18E-27	13. <b>EIF2AK2</b>	2,05518913	3,67E-51
14. <b>ARNTL2</b>	-1,6887385	1,93E-25	14. <b>EPB41L5</b>	1,6763618	6,20E-50
15. <b>P2RY14</b>	-2,2532221	2,78E-24	15. <b>SELL</b>	1,73757504	1,17E-48
16. <b>CCDC28A</b>	-1,2184364	5,37E-24	16. <b>MX1</b>	2,84169448	2,73E-47
17. <b>LDLRAD4</b>	-1,0044388	6,27E-23	17. <b>ISG15</b>	2,53343526	4,53E-47
18. <b>RDH10</b>	-2,2193282	1,40E-22	18. <b>SAMD9L</b>	1,83900334	6,85E-47
19. <b>CXCR6</b>	-2,9912327	1,46E-22	19. <b>DTX3L</b>	1,63542121	3,04E-46
20. <b>ITGAE</b>	-1,0243546	3,10E-22	20. <b>BST2</b>	1,43044376	4,14E-45
21. <b>GSTP1</b>	-1,1368922	7,78E-22	21. <b>PYHIN1</b>	1,63198905	6,47E-45
22. <b>SRXN1</b>	-1,6506528	1,29E-21	22. <b>DHX58</b>	1,67590179	1,09E-44
23. <b>TALDO1</b>	-1,6267585	3,36E-21	23. <b>TRIM25</b>	1,17836377	1,34E-44
24. <b>CREM</b>	-1,3582741	9,38E-21	24. <b>IFIT1</b>	3,95532666	5,36E-43
25. <b>GCLM</b>	-1,1804538	1,94E-19	25. <b>NEXN</b>	1,98919938	1,81E-42



**Table S6:** The 1,000 genes with the highest average normalized count across all samples, used to construct the heat map in **Figure 4A** (excel file).

## SUPPLEMENTAL EXPERIMENTAL PROCEDURES

**Statistical analysis for RNA Sequencing:** Reads shorter than 20 bp after the trimming were removed. The remaining reads were aligned to the human genome (hg19) with TopHat2 (Version 2.0.9) (Kim et al., 2013). A gtf file from the Illumina iGenomes project ([https://support.illumina.com/sequencing/sequencing\\_software/igenome.ilmn](https://support.illumina.com/sequencing/sequencing_software/igenome.ilmn)), defining the gene models, was supplied to TopHat2. htseq-count was used to quantify the number of reads mapping to each gene in the gtf file, using the 'union' counting mode to handle reads overlapping several genes (Anders et al., 2014). All genes with zero counts in all samples were excluded, leaving in total 21,481 genes for further interrogation. For exploratory analysis (heat map, hierarchical clustering and principal components analysis), we transformed the counts by use of the regularized log transformation in the DESeq2 R package (Version 1.2.10) (Love et al., 2014). The transformed values for each gene were further standardized by subtraction of the mean value and division by the standard deviation across all samples. Differential expression analysis was performed on the count data by DESeq2 with default settings. To visually compare the expression levels of genes across different conditions, we used the normalized counts calculated with DESeq2.

The “stem cell genes” for GSEA can be found under the following link (04/2015):

[http://www.sabiosciences.com/Stem\\_Cell.php](http://www.sabiosciences.com/Stem_Cell.php)

Tested genes were: *APC*, *AXIN1*, *CCNA2*, *CCND1*, *CCND2*, *CCNE1*, *CDK1*, *CDC42*, *EP300*, *FGF2*, *MYC*, *NOTCH2*, *PARD6A*, *RBI*, *KAT2A*, *HDAC2*, *KAT8*, *KAT7*, *TERT*, *NOTCH1*, *NUMB*, *HSPA9*, *SOX2*, *BMP1*, *BMP2*, *BMP3*, *IGF1*, *JAG1*, *DLL1*, *GJAI*, *CD4*, *CD44*, *CDH1*, *CDH2*, *COL9A1*, *CTNNA1*, *NCAM1*, *ABCG2*, *ALDH2*, *FGFR1*, *FOXA2*, *MSX1*, *CD3D*, *CD8A*, *CD8B*, *MME*, *ACAN*, *COL1A1*, *COL2A1*, *PPARG*, *SIGMAR1*, *S100B*, *TUBB3*, *DTX1*, *DTX2*, *DVL1*, *ADAR*, *BTRC*, *FRAT1*, *FZD1*, *PPARD*, *WNT1*

## Staining panels

### Staining panel for T<sub>N</sub> cell sorting and T<sub>SCM</sub> cell assessment in humans.

Marker	Fluorochrome	Clone	Isotype	Vendor
CD3	A700	HIT3a	Mouse IgG2a, κ	BioLegend
CD4	Pacific Blue	13B8.2	Mouse IgG1	Beckman Coulter
(CD4)	(PE)	(13B8.2)	(Mouse IgG1)	(Beckman Coulter)
CD8	APC-A750	B9.11	Mouse IgG1	Beckman Coulter
CCR7	PerCP-Cy5.5	TG8/CCR7	Mouse IgG2a, κ	BioLegend
(CCR7)	(Brilliant Violet)	(G043H7)	(Mouse IgG2a, κ)	(BioLegend)
CD45RA	ECD	2H4LDH11LDB9	Mouse IgG1	Beckman Coulter
CD95	APC	DX2	Mouse IgG1, κ	BioLegend
CD58	FITC	1C3	Mouse IgG2a, κ	BD Biosciences
Dead cells	Vivid Aqua	Not specified	Not specified	Life Technologies

### Staining panel for T<sub>N</sub> cell sorting and T<sub>SCM</sub> cell assessment in mice.

Marker	Fluorochrome	Clone	Isotype	Vendor
CD3e	A700	17A2	Rat IgG2b, κ	eBioscience
CD4	FITC	GK1.5	Not specified	In house
CD8a	Pe-AlexaFluor610	5H10	RatIgG2b	Invitrogen
CD62L	PE	Mel14	Rat IgG2a, κ	eBioscience
CD44	APC-eFluor780	1M7	Rat IgG2b, κ	eBioscience
CD122	eFluor 450	TM-b1	Rat IgG2b	eBioscience
CXCR3	APC	CXCR3-173	Armenian Hamster IgG	BioLegend
Sca-1	Pe-Cy7	D7	Rat IgG2a, κ	eBioscience
Dead cells	7-AAD	-	-	BioLegend

### Staining panel for T<sub>N</sub> cell sorting for phospho-specific flow cytometry.

Marker	Fluorochrome	Clone	Isotype	Vendor
CD3	A700	HIT3a	Mouse IgG2a, κ	BioLegend
CD4	Pacific Blue	13B8.2	Mouse IgG1	Beckman Coulter
CD8	APC-A750	B9.11	Mouse IgG1	Beckman Coulter
CCR7	PerCp-Cy5.5	TG8/CCR7	Mouse IgG2a, κ	BioLegend
CD45RA	ECD	2H4LDH11LDB9	Mouse IgG1	Beckman Coulter
CD95	APC	DX2	Mouse IgG1, κ	BioLegend
CD58	FITC	1C3	Mouse IgG2a, κ	BD Biosciences
Dead cells	Vivid Aqua	Not specified	Not specified	Life Technologies

### Staining panel for CFSE dilution assay.

Marker	Fluorochrome	Clone	Isotype	Vendor
Cell proliferation	Cell Trace Violet	Not specified	Not specified	LifeTechnologies
CD3	A700	HIT3a	Mouse IgG2a, κ	BioLegend
CD4	PE	13B8.2	Mouse IgG1	Beckman Coulter
CD8	PE-Cy7	SK1	Mouse IgG1, κ	BD Biosciences
CCR7	PerCp-Cy5.5	TG8/CCR7	Mouse IgG2a, κ	BioLegend
CD45RA	ECD	2H4LDH11LDB9	Mouse IgG1	Beckman Coulter
CD95	APC	DX2	Mouse IgG1, κ	BioLegend
CD58	FITC	1C3	Mouse IgG2a, κ	BD Biosciences
Dead cells	Vivid Near	Not specified	Not specified	LifeTechnologies

### Staining panel for TMRE assessment.

Marker	Fluorochrome	Clone	Isotype	Vendor
MMP	TMRE	Not specified	Not specified	MitoScience
CD3	PerCP-Cy5.5	UCHT1	Mouse IgG1, κ	BioLegend
CD4	PE-Cy7	SK3	Mouse IgG1, κ	BD Biosciences
CD8	APC-A750	B9.11	Mouse IgG1	Beckman Coulter
CCR7	Brilliant Violet	G043H7	Mouse IgG2a, κ	BioLegend
CD45RA	A700	HI100	Mouse IgG2b, κ	BD Biosciences
CD95	APC	DX2	Mouse IgG1, κ	BioLegend
CD58	FITC	1C3	Mouse IgG2a, κ	BD Biosciences
Dead cells	Vivid Aqua	Not specified	Not specified	Life Technologies

### Staining panel for assessment of 2-NBDG uptake.

Marker	Fluorochrome	Clone	Isotype	Vendor
2-NBDG	Fluorescein	Not specified	Not specified	LifeTechnologies
CD3	A700	HIT3a	Mouse IgG2a, κ	BioLegend
CD4	PE-Cy7	SK3	Mouse IgG1, κ	BD Biosciences
CD8	APC-A750	B9.11	Mouse IgG1	Beckman Coulter
CCR7	Brilliant Violet 421	G043H7	Mouse IgG2a, κ	BioLegend
CD45RA	ECD	2H4LDH11LDB9	Mouse IgG1	Beckman Coulter
CD95	PE-Cy7	DX2	Mouse IgG1, κ	BioLegend
CD58	APC	TS2/9	Mouse IgG1	eBioscience
Dead cells	Vivid Aqua	Not specified	Not specified	Life Technologies

**Staining panel for KLF2 assessment.**

<b>Marker</b>	<b>Fluorochrome</b>	<b>Clone</b>	<b>Isotype</b>	<b>Vendor</b>
KLF2	Alexa488	Polyclonal	Rabbit IgG	BIOSS
CD3	A700	HIT3a	Mouse IgG2a, κ	BioLegend
CD4	PE-Cy7	SK3	Mouse IgG1, κ	BD Biosciences
CD8	APC-A750	B9.11	Mouse IgG1	Beckman Coulter
CCR7	Brilliant Violet 421	G043H7	Mouse IgG2a, κ	BioLegend
CD45RA	ECD	2H4LDH11LDB9	Mouse IgG1	Beckman Coulter
CD95	PE-Cy7	DX2	Mouse IgG1, κ	BioLegend
CD58	APC	TS2/9	Mouse IgG1	eBioscience
Dead cells	Vivid Aqua	Not specified	Not specified	Life Technologies

## **SUPPLEMENTAL REFERENCES**

Anders, S., Pyl, P.T., and Huber, W. (2014). HTSeq A Python framework to work with high-throughput sequencing data.

Kim, D., Pertea, G., Trapnell, C., Pimentel, H., Kelley, R., and Salzberg, S.L. (2013). TopHat2: accurate alignment of transcriptomes in the presence of insertions, deletions and gene fusions. *Genome Biol.* *14*, R36.

Love, M.I., Huber, W., and Anders, S. (2014). Moderated estimation of fold change and dispersion for RNA-Seq data with DESeq2.